

Parametric dependence of fast-ion transport events on the National Spherical Torus Experiment

This content has been downloaded from IOPscience. Please scroll down to see the full text.

2014 Nucl. Fusion 54 093007

(<http://iopscience.iop.org/0029-5515/54/9/093007>)

View [the table of contents for this issue](#), or go to the [journal homepage](#) for more

Download details:

IP Address: 198.125.233.17

This content was downloaded on 05/01/2015 at 20:50

Please note that [terms and conditions apply](#).

Parametric dependence of fast-ion transport events on the National Spherical Torus Experiment

E.D. Fredrickson¹, N.N. Gorelenkov¹, M. Podesta¹, A. Bortolon², S.P. Gerhardt¹, R.E. Bell¹, A. Diallo¹ and B. LeBlanc¹

¹ Princeton Plasma Physics Laboratory, Princeton, NJ 08543, USA

² Department of Nuclear Engineering, University of Tennessee, Knoxville, TN 37916, USA

E-mail: efredrickson@pppl.gov

Received 21 March 2014, revised 6 June 2014

Accepted for publication 17 July 2014

Published 15 August 2014

Abstract

This paper presents an empirical approach towards characterizing the stability boundaries for some common energetic-ion-driven instabilities as seen on the National Spherical Torus Experiment (NSTX). Understanding the conditions for which beam-driven instabilities arise, and the extent of the resulting perturbation to the fast-ion population, is important for predicting and eventually demonstrating non-inductive current ramp-up and sustainment in NSTX-U (Menard J. *et al* 2012 *Nucl. Fusion* **52** 083015), as well as the performance of future fusion plasma experiments such as ITER. A database has been constructed, based on shots from the 2010 experimental campaign for which TRANSP runs were performed. Each shot was divided into 50 ms intervals and the dominant beam-driven activity was characterized, and plasma parameters were collected into a database. It is found that TAE avalanches are present for $\beta_{\text{fast}}/\beta_{\text{total}} > 0.3$ and quiescent plasmas only for $\beta_{\text{fast}}/\beta_{\text{total}} < 0.3$.

Keywords: energetic particles, TAE, NSTX

(Some figures may appear in colour only in the online journal)

1. Introduction

The ability to predict the confinement and energy transfer rate of fast ions to the thermal plasma is important for accurate modelling of beam-driven currents that ITER and spherical tokamaks (STs) rely upon. National Spherical Torus Experiment (NSTX) plasmas can have fast-ion redistribution events caused by toroidal or global Alfvén eigenmode (TAE/GAE) avalanches or fishbone-like energetic particle modes (EPMs) [1–6], periods without significant fast-ion redistribution events, but with many modes, or quiescent periods with weak mode activity. The identification of plasma parameters that empirically affect the stability of modes excited by energetic particles will help us to guide experiments and provide valuable input for developing theoretical models to predict the (possibly non-linear) fast-ion redistribution from these instabilities (figure 1).

Present theoretical understanding of TAE stability suggests parameters that might be correlated with fast-ion redistribution events. The fast-ion beta is a measure of the drive for the EPM, TAE and GAE. Landau damping, an important damping mechanism, is proportional to the ion and electron thermal beta, suggesting that the dimensionless parameter $\beta_{\text{fast}}/\beta_{\text{total}}$ is an important parameter governing,

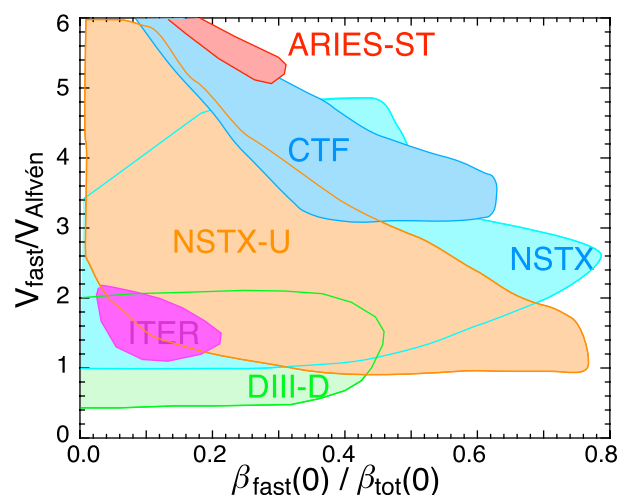


Figure 1. Map of NSTX operational space in terms of the fast-ion β normalized to the total β , and the fast-ion velocity normalized to the Alfvén speed.

at least, Alfvénic fast-ion-driven instability behaviour. The ratio of β_{fast} to β_{thermal} (equivalent to β_{fast} to β_{total}) is, in an equilibrium plasma dominated by fast-ion heating, roughly

equivalent to the ratio of the fast-ion slowing-down time, τ_{slow} , to the thermal energy confinement time, τ_E . In a similar sense, the dimensionless number giving the ratio of the fast-ion injection velocity to the Alfvén speed, $V_{\text{fast}}/V_{\text{Alfvén}}$, is a measure of the fraction of fast ions in the resulting slowing-down distribution, which can be resonant with the Alfvénic modes. The ratio of orbit size to plasma minor radius is another important parameter in the context of fast-ion transport physics. However, the range of that parameter is small in this dataset, $0.14 < \rho_{\text{Larmor}}/a_{\text{plasma}} < 0.41$, and no meaningful dependences on this parameter have yet been found. Other parameters, more difficult to measure, such as those associated with the q -profile (e.g. q_{min}), or parameters describing the fast-ion distribution (e.g. anisotropy) are also clearly important. Finding q -profile dependences requires very labour-intensive equilibrium reconstructions, which are ongoing and may, in the future, provide some useful scaling information.

In this paper, we describe the construction of a database of these plasma parameters, coupled with a characterization of the mode activity at these times. In this parameter space we will show that the existence of TAE avalanches, GAE avalanches and quiescent plasmas is constrained to certain ranges of parameters on NSTX.

2. Experimental approach

The fast-ion beta, an important parameter in this study, is not directly measured in NSTX. At present, the fast-ion beta is calculated from the time evolution of plasma parameters such as density and electron temperature in each discharge, assuming only classical collisional processes. The resulting fast-ion beta should be regarded as an approximate maximum, which could be degraded by many different forms of magnetohydrodynamic (MHD) activity, or possibly even by plasma turbulence. This calculation is typically done with the NUBEAM code [7] in TRANSP [8]; thus, the initial part of this study was limited to NSTX shots for which TRANSP runs had been done. The database was constructed from ≈ 360 TRANSP runs on shots from the 2010 experimental campaign on NSTX. The database was constructed by dividing each TRANSP run into 50 ms intervals, starting at 150 ms and characterizing the type of MHD activity in the interval. Typically, by 150 ms NSTX plasmas have reached a plasma current of ≈ 0.6 – 0.7 MA, and fast-ion confinement is reasonably good. The 50 ms time interval is several fast-ion slowing-down times, and is typically comparable to the timescale for evolution of MHD phenomena. The average density, the energy stored in the fast-ion population, the plasma total stored energy and the maximum beam injection voltage for each 50 ms interval are extracted from the data stored in the TRANSP output files. The plasma density, together with the on-axis magnetic field, is used to calculate an effective Alfvén velocity and the beam voltage is used to calculate the maximum beam ion velocity, from which the normalized fast-ion velocity, $V_{\text{fast}}/V_{\text{Alfvén}}$, is calculated.

The majority of these shots are in H-mode, although the parameters for these shots vary significantly. The range of plasma currents is from 0.3 up to 1.3 MA, with an average value of 0.9 MA. The plasmas are heated with up to 6 MW of neutral beam power (three sources, each capable of injecting powers of

up to 2 MW at 90 kV), with the maximum (and typical) beam voltage of 90 kV. The on-axis magnetic field varies from 2.7 up to 5.3 kG. The electron density typically increases throughout each shot, and the central densities range from 0.9×10^{13} up to $1.3 \times 10^{14} \text{ m}^{-3}$. The central electron temperature is typically ≈ 0.9 keV, but in this dataset ranges from 0.23 up to 1.7 keV.

The MHD activity in each 50 ms interval is classified as having TAE avalanches, bursting TAE, constant-amplitude TAE, EPMS, GAE avalanches, abrupt large events (ALEs) [9–11] or plasmas quiescent in the TAE and lower frequency range. As the kink modes are believed to redistribute fast ions, intervals with kink modes in addition to the fast-ion-driven MHD events are counted as ‘kinks’. Intervals with GAE avalanches are counted independently of any other classification of the interval.

The distinction between TAE avalanches, EPMS and ALEs is not as unambiguous on NSTX as it is on conventional aspect ratio tokamaks. The low-field (typically 0.4 T), high-density, $n_e(0)$ up to $1.3 \times 10^{14} \text{ m}^{-3}$, and unbalanced co-injected beams typically result in a core rotation frequency ≈ 25 – 30 kHz on the axis, comparable to the TAE gap frequency. For modes with a moderate toroidal mode number, $n = 2$ – 4 , the Doppler-corrected TAE frequency is often near zero in the plasma frame near the magnetic axis, allowing direct coupling of TAE to EPM or other core MHD modes (see figure 5, [1] where the Doppler-corrected frequency of the $n = 2$ TAE becomes negative in the plasma core). That is, the TAE frequency range overlaps the frequency range of EPMS and kink modes.

Representative examples of a TAE avalanche, EPM and ALE are shown in figure 2. In the first frame, the strong burst of activity (peak rms amplitude of ≈ 12 G) is preceded by weaker modes (≈ 2 G) with frequencies consistent with the TAE frequencies calculated by the NOVA code [12–14]. The modes in the strong burst chirp down to low frequencies, but at mode onset, they are in the TAE frequency range. In the second frame is an example of a mode burst with both TAE avalanche and EPM characteristics. The mode onset frequency appears to be in the TAE gap; the modes chirp to a low frequency, but the post-burst frequency evolution is more consistent with ideal kink-like modes, suggesting that the TAE couple to (and sometimes trigger) a core kink-like mode. The third frame shows a typical EPM avalanche, where the mode onset frequency is well below the (core) TAE frequency band and the harmonic spacing is consistent with kink-like modes. In the final frame is a burst reminiscent of the ALEs reported on the JT-60U experiment. The spectrogram does suggest very rapid downward frequency chirping, and the ALEs on NSTX are likely just an example of extremely fast chirping TAE avalanches. In the rest of the paper, TAE avalanches and the ALE-like events will both be classified as TAE avalanches.

3. Experimental results

Some data from the database are shown in figure 3. Each point in the figure represents a 50 ms interval in one of the 360 shots comprising the database. The colour of the point indicates the type of instability dominant in that interval. In figure 3, points are labelled quiescent if there is no detectable TAE, EPM or kink activity but most quiescent points would have higher frequency GAE or CAE activity. If a kink (or tearing

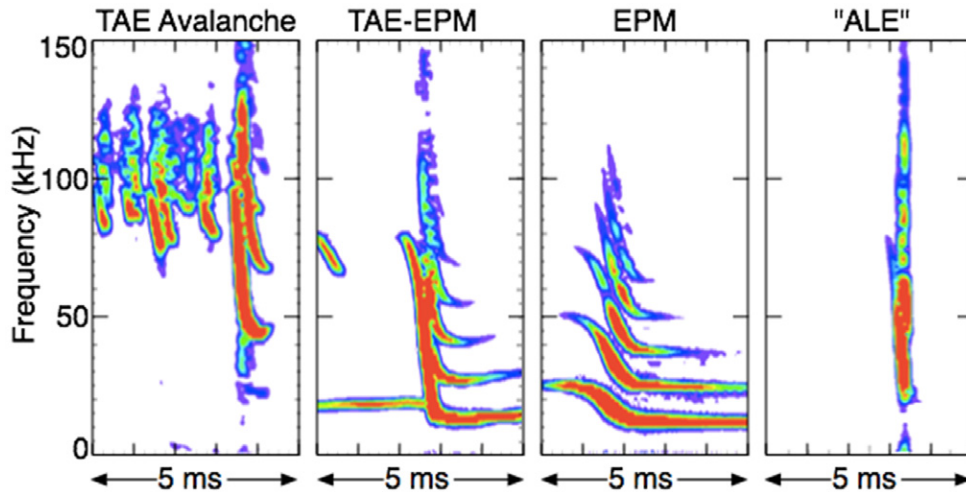


Figure 2. (a) Spectrogram showing a TAE avalanche, (b) spectrogram showing a hybrid TAE avalanche and EPM, (c) spectrogram of an EPM avalanche and (d) spectrogram of an ALE.

mode) is present, the interval is labelled ‘kink’ and other types of instabilities which might be present are ignored. Bursting or constant wave TAE can exist between TAE avalanche events, but intervals containing TAE avalanches are labelled only as avalanches. TAE avalanches often interact strongly with EPM, and those events are labelled as EPM.

The horizontal axis is the ratio of the fast-ion beta, β_{fast} , to the total plasma beta, β_{total} . The vertical axis is the ratio of the birth velocity of the full-energy beam ions normalized to an average Alfvén speed. The Alfvén speed is calculated using the magnetic field on the magnetic axis, and the line average of the plasma electron density inside the pedestal (from a major radius of 0.3 to 1.4 m). Other choices for the axis, for example, using more core-localized values, would result in small qualitative changes to this graph, but there is probably a high degree of self-similarity in these NSTX discharges that would make the results insensitive to those changes.

Each point in figure 3 shows the ratio of the fast-ion velocity to an effective Alfvén speed where the fast-ion velocity is calculated at the maximum injection energy. The neutral beams on NSTX also inject substantial power in fast ions at the half and third energies. Together, the injected energetic ions collisionally slow down in the plasma, resulting in a non-thermal slowing-down distribution. The combined slowing-down and thermal ion distributions are nearly Maxwellian at energies below the thermal ion temperature, and non-Maxwellian at much higher energy. The energy above which the combined distribution is significantly non-Maxwellian depends on parameters such as the relative number density of fast ions to thermal ions and the thermal ion temperature, but for these NSTX plasmas, above roughly 5–10 keV, the ion distribution becomes significantly non-Maxwellian.

Generally, NSTX shots evolve, starting from the lower right of figure 3 and moving upwards and to the left as the plasma density increases. The increasing density lowers the Alfvén speed, increasing $V_{\text{fast}}/V_{\text{Alfvén}}$, and the higher density decreases the fast-ion slowing-down time, dropping the fast-ion stored energy. At the same time, the density rise generally coincides with an increase in the thermal plasma stored energy or β_{total} . Thus, there can be hidden correlations in these figures

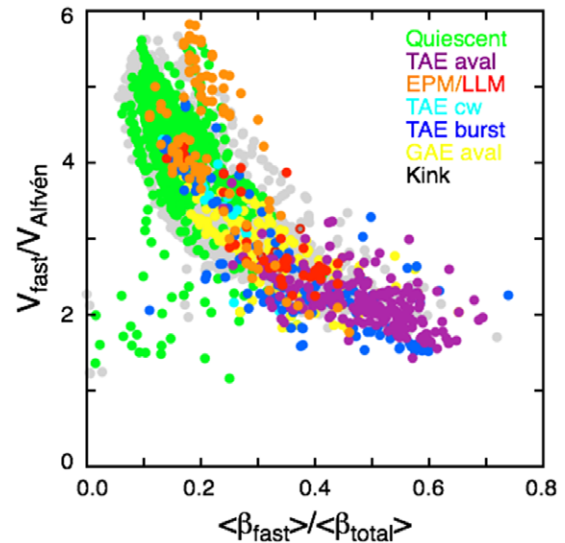


Figure 3. Existence plot for a variety of MHD activities.

as, for example, points in the lower right tend to be from early in the shot and would tend to have elevated q_{min} and typically core shear reversal.

The quiescent discharge periods, and periods with TAE avalanches are well localized in this parameter space. In figure 4 the quiescent period data (green points) are plotted. There does not seem to be a strong dependence on the normalized fast-ion velocity, but quiescent plasmas mostly have a ratio of fast-ion stored energy to total stored energy of less than $\approx 30\%$. Conversely, the TAE avalanche events occur where that ratio $\beta_{\text{fast}}/\beta_{\text{total}} > 0.3$. Again, within this dataset, there does not seem to be a significant dependence on $V_{\text{fast}}/V_{\text{Alfvén}}$. Even the L-mode avalanches, with lower voltage beams (60–70 keV), fall into the same region.

Many shots have TAE activity below the threshold for causing measurable transient drops in the neutron rate. These tend to be distributed fairly uniformly as can be seen in figure 5. Here, the presence of bursting and chirping TAEs is indicated by blue points and TAEs with a more continuous amplitude

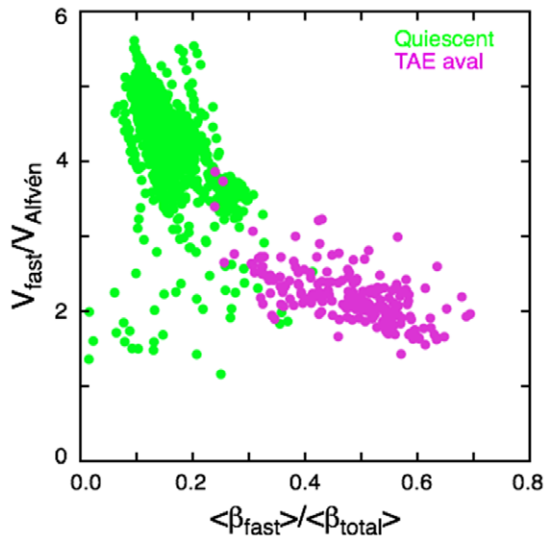


Figure 4. Distribution of quiescent shots (green), and shots with TAE avalanches (purple) and ALEs (magenta).

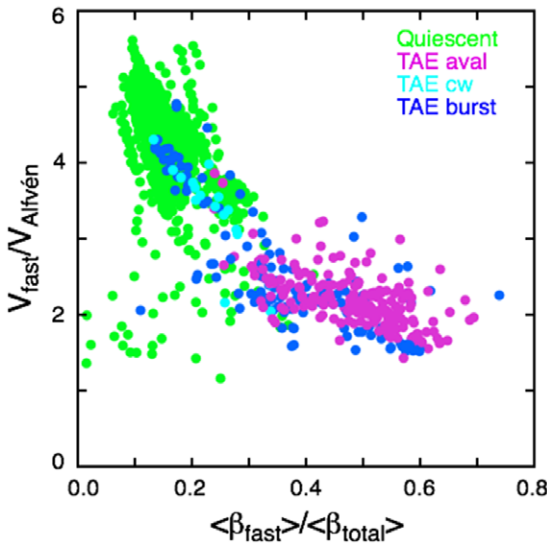


Figure 5. Distribution of shots with bursting and chirping TAEs (blue) and continuous amplitude TAEs (cyan).

evolution are indicated by cyan. The bursting and chirping TAEs overlap the TAE avalanching region, and also extend into the parameter space where quiescent plasmas are found. The continuous TAEs mostly overlap the quiescent regime and appear to be weaker modes. In NSTX plasmas, the thermal neutron production is negligible; neutrons from beam–target and beam–beam reactions dominate. Thus, the neutron rate is a sensitive measure of changes in the fast-ion distribution.

The second type of instability most commonly responsible for fast-ion redistribution events on NSTX are EPMS. These instabilities are not eigenmodes of the plasma, excited by a non-thermal particle population, but exist only in the presence of an energetic particle (ion) population. Their frequencies are a characteristic of the energetic fast-ion population. There are many qualitatively different low-frequency chirping modes that are classified as EPMS on NSTX. However, a large fraction of these bursts are of the types shown in figures 6 and 7.

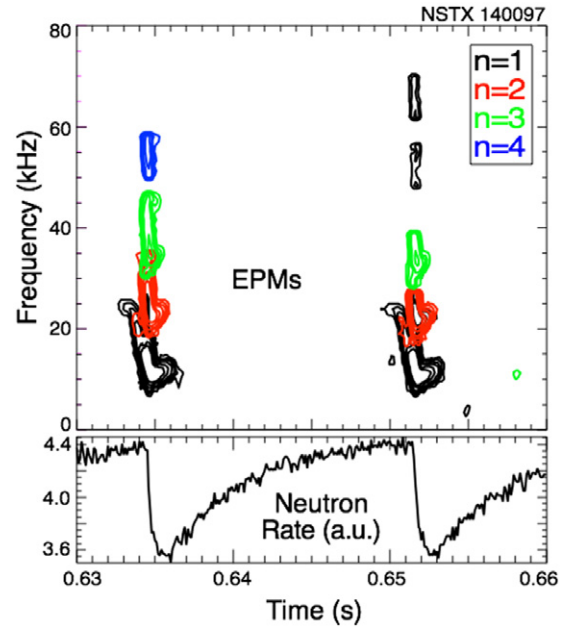


Figure 6. Fishbone-like EPMS in the later part of the NSTX discharge. Coupling of $n = 1$ to higher n 's is commonly seen.

Figure 6(a) shows typical EPM bursts as seen in the latter part of the discharge, although bursts like these may appear early, as well. They resemble the classical fishbone modes seen on conventional tokamaks, and like those, appear when q_{min} or $q(0)$ is near unity. They may be accompanied by substantial, but transient, drops in the neutron rate, as seen in figure 6(b). Typically on NSTX, the bursts involve multiple toroidal mode numbers, as indicated in figure 6(a) by the coloured contours.

In figure 7 is shown an example of the second common form of EPM. The multiple toroidal mode numbers, and the relatively small frequency chirps are very similar to the EPMS in figure 6. However, these EPMS, which are typically seen early in the discharge when q_{min} is still elevated, convert to long-lived modes [15, 16]. As the duration of the long-lived mode varies considerably, the distinction between the types can be somewhat arbitrary.

In figure 8 are shown the EPM points (orange, red and blue), overlaid on the quiescent regime (green points) and kink-like modes (grey). Here, the two subgroups of EPM from above are separately identified. In blue are EPMS that closely resemble classical fishbones and in red are EPMS coupled to the long-lived mode. The orange points represent EPMS that are not easily sorted into the above categories. EPMS and kinks are of course related as the EPM is, generically, a stable kink mode destabilized by a resonance with fast ions. The fast frequency chirp of EPMS is used to discriminate between them and kink modes. However, many long-lived kinks on NSTX begin with a quick downward frequency chirp similar to the long-lived modes on MAST [15, 16], which suggests that fast-ion resonances may play a role in maintaining their saturated state.

The EPMS tend to be more core-localized than the TAE, thus $\beta_{fast}(0)/\beta_{total}(0)$ might be a more appropriate parameter than the one using volume-averaged β 's. In figure 9 is an existence plot for the EPM against the central and volume-averaged ratios of the fast ion to the total pressures. The

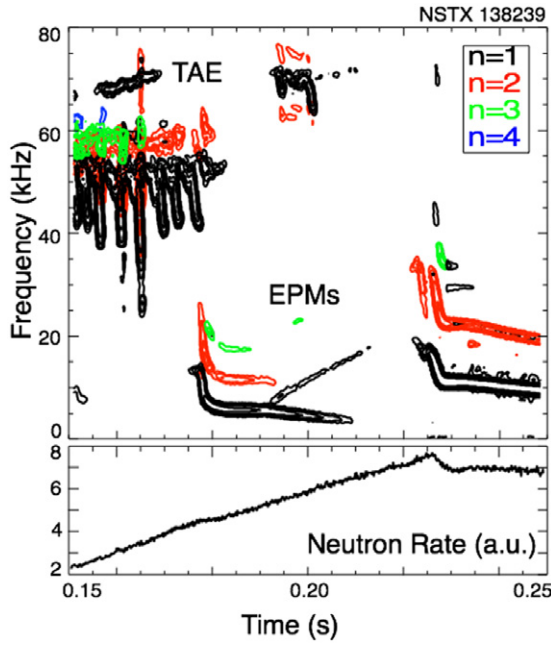


Figure 7. Fishbone-like EPMs coupled to long-lived modes: (a) spectrogram of Mirnov coil signal, (b) neutron rate.

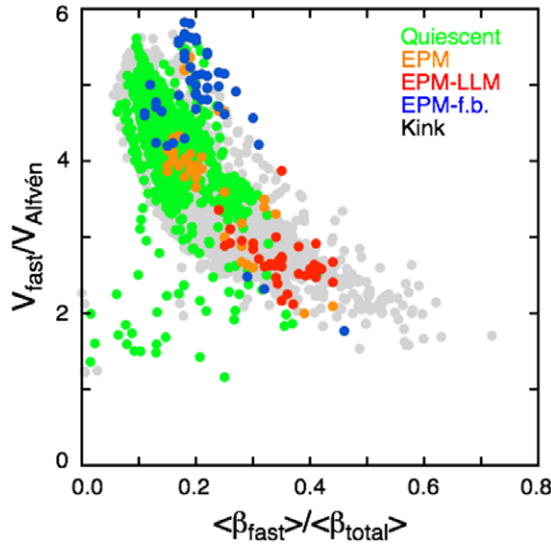


Figure 8. EPM events (orange) are seen over most of the NSTX operating space, as are low-frequency kink-like modes (grey).

first observation is that these two parameters are fairly well correlated, which indicates that the ratio of the peaking factors for the fast-ion pressure profile and the total pressure profile are correlated. In terms of the core parameters, EPM appear to be absent for $\beta_{fast}(0)/\beta_{total}(0) < 0.2$, or similarly, for $\langle \beta_{fast} \rangle / \langle \beta_{total} \rangle < 0.1$. The solid line indicates where the fast-ion pressure peaking factor is twice that of the total pressure. The upper and lower dashed lines correspond to peaking factor ratios of 2.5 and 1.5, respectively.

This choice of normalized fast-ion velocity and normalized fast-ion beta also works reasonably well for predicting conditions under which GAE avalanches are seen. GAE avalanches have not, so far, resulted in measurable neutron rate drops, but there are direct and indirect indications

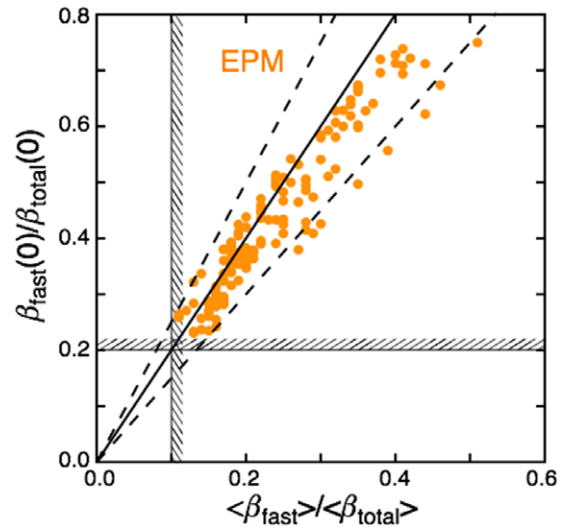


Figure 9. EPM existence plot in the parameter space of $\beta_{fast}(0)/\beta_{total}(0)$ versus $\langle \beta_{fast} \rangle / \langle \beta_{total} \rangle$. Solid line indicates β_{fast} peaking factor twice β_{total} peaking factor.

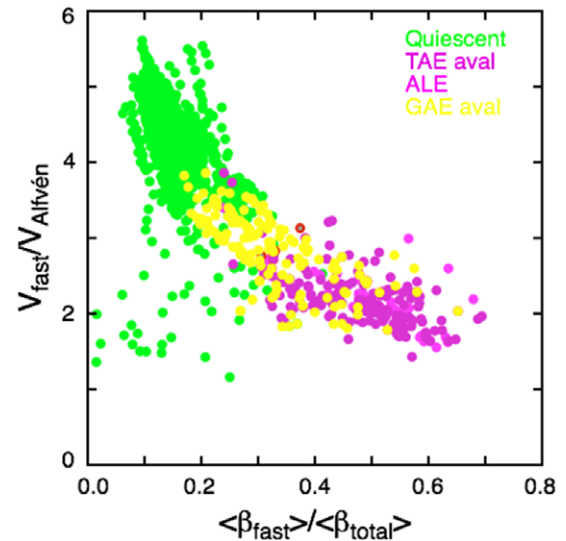


Figure 10. Yellow points indicate parameters for which GAE avalanches were seen.

of fast-ion redistribution due to GAE avalanches [17]. In figure 10 is shown the region where GAE avalanches are found. They extend down to lower $\beta_{fast}/\beta_{total}$ than the TAE avalanches, and there may also be a cutoff for $V_{fast}/V_{Alfvén}$ greater than ≈ 3.5 .

Predictive TRANSP runs were performed to simulate NSTX-U performance using the neutral beam parameters and machine parameters (plasma current, toroidal field, vacuum vessel configuration) expected for NSTX-U [18]. The TRANSP runs explored a range of parameters, including different combinations of neutral beam sources, and scans of density and toroidal field. Using those predictive TRANSP runs, we can compare the expected operational space of NSTX-U with the NSTX data presented above. Figure 11 shows the data from these TRANSP runs, analysed in the same manner as above. Data from the NSTX-U TRANSP runs are shown in black, and are overlaid by the quiescent and TAE avalanching

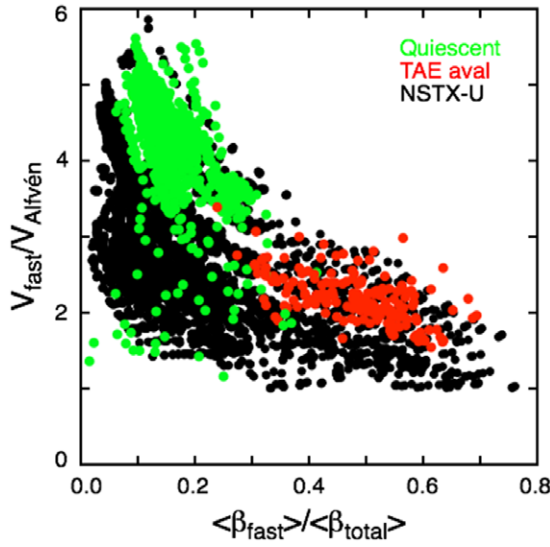


Figure 11. Operational space for NSTX-U as predicted with TRANSP (black), overlaid by data from NSTX.

data points from NSTX. As can be seen, NSTX-U should be able to access parameters which were found to be quiescent on NSTX, as well as parameters where TAE avalanching might be expected. NSTX-U will also extend the operational space to much lower $V_{fast}/V_{Alfvén}$.

4. Scaling of the transient neutron rate drops

The neutron rate transiently drops during each TAE avalanche or EPM event. The neutron rate drop is due to fast-ion redistribution, fast-ion losses and to energy transferred from the fast ions through the mode to the thermal plasma. A prediction of the neutron rate drop is complicated, and depends on the structure of the modes, the mode frequency and amplitude evolution, the initial fast-ion distribution, and other parameters. Here, we look at the empirical scaling of neutron rate drops versus a single parameter, the peak mode amplitude as measured by a Mirnov coil. In figure 12 is shown a plot of the drop in neutron rate versus the peak amplitude of the TAE avalanche. The neutron rate drops follow an offset-linear scaling with mode amplitude, suggesting an amplitude threshold for the onset of the avalanche. This is consistent with fast-ion transport simulations during avalanches, which also found a threshold in amplitude, both for significant fast-ion energy loss and redistribution, and a higher threshold still for fast-ion losses [1]. As the TAE avalanche amplitude drops, the change in neutron rate becomes smaller, until the neutron rate change becomes comparable to the noise level.

In figure 13 is shown the scaling of neutron rate drops due to fishbone-like EPM and EPM coupled to long-lived modes, together with the scaling for TAE bursts (now shown in green), as in figure 12. The peak EPM edge magnetic fluctuation level tends to be larger than that for TAE avalanches for similar drops in the normalized neutron rate. There is enough scatter in the data to make it clear that parameters in addition to the edge mode amplitude play a role in the magnitude of the neutron rate drop. The scaling of the neutron rate drop with edge magnetic fluctuation amplitude is similar for the two types of fishbone-like EPMS, although there is considerably more scatter for the

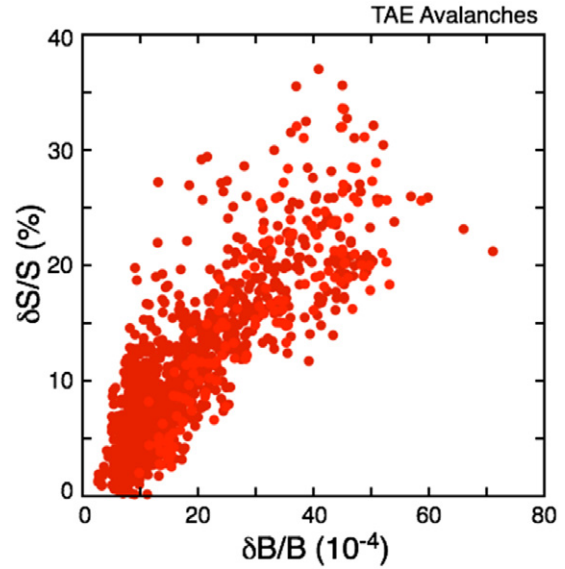


Figure 12. Drop in neutron rate versus peak edge magnetic fluctuation amplitude for TAE avalanches.

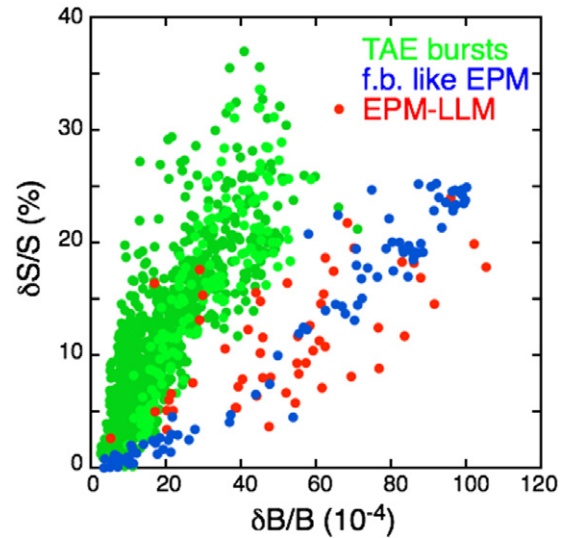


Figure 13. Scaling of neutron rate drops with edge magnetic fluctuation amplitude for TAE (green), fishbone-like EPM (blue) and EPM coupled to long-lived modes (red).

EPM coupled to the long-lived mode, perhaps reflecting more variability in the plasma conditions at the time of these events.

5. Summary

The dependence of energetic particle driven mode activity on plasma global parameters has been studied in NSTX. On NSTX, two fast-ion instabilities are predominantly responsible for fast-ion redistribution events, the TAE avalanches and fishbone-like energetic particle modes. Understanding the conditions under which beam-driven instabilities arise, and the extent of the resulting perturbation to the fast-ion population, is important for predicting and eventually demonstrating non-inductive current ramp-up and sustainment in NSTX-U, as

well as for predicting the performance of future fusion plasma experiments such as ITER. A database has been constructed for each 50 ms interval from a representative selection of ≈ 360 shots. The database includes some basic, global plasma parameters, as well as the identification of the dominant mode activity in each interval. It has been shown that for this NSTX data set, TAE avalanching is only seen when the calculated $\beta_{\text{fast}}/\beta_{\text{total}} > 0.3$, and conversely, that quiescent plasmas are only seen for $\beta_{\text{fast}}/\beta_{\text{total}} < 0.3$.

The fast-ion losses for both TAE avalanches and EPMS scale roughly linearly with mode amplitude as measured with Mirnov coils. This linear scaling is similar to what has been reported for losses resulting from TAE bursts on TFTR [19], although the offset-linear scaling seen here for TAE avalanches was not seen on TFTR.

Acknowledgments

The authors would like to express their appreciation to the NSTX team for performing the experiments from which these data were collected. This paper has been authored under US DoE Contract Number DE-AC02-09CH11466.

References

- [1] Fredrickson E.D. *et al* 2013 Fast-ion energy loss during TAE avalanches in the National Spherical Torus Experiment *Nucl. Fusion* **53** 013006
- [2] Fredrickson E.D., Chen L. and White R.B. 2003 Bounce precession fishbones in the National Spherical Torus Experiment *Nucl. Fusion* **43** 1258
- [3] Fredrickson E.D. *et al* 2003 *Phys. Plasmas* **10** 2852
- [4] Podestà M. *et al* 2009 *Phys. Plasmas* **16** 056104
- [5] Darrow D.S., Crocker N., Fredrickson E.D., Gorelenkov N.N., Gorelenkova M., Kubota S., Medley S.S., Podestà M., Shi L. and White R.B. 2013 Stochastic orbit loss of neutral beam ions from NSTX due to toroidal Alfvén eigenmode avalanches *Nucl. Fusion* **53** 013009
- [6] Podestà M. *et al* 2012 Study of chirping TAEs on the National Spherical Torus Experiment *Nucl. Fusion* **52** 094001
- [7] Pankin A. *et al* 2004 *Comput. Phys. Commun.* **159** 157–84
- [8] Budny R.V. 1994 *Nucl. Fusion* **34** 1247
- [9] Shinohara K. *et al* and the JT-60 Team 2001 *Nucl. Fusion* **41** 603
- [10] Shinohara K. *et al* and the JT-60 Team 2002 Recent progress of Alfvén eigenmode experiments using N-NB in JT-60U tokamak *Nucl. Fusion* **42** 942
- [11] Shinohara K. *et al* 2004 Energetic particle physics in JT-60U and JFT-2M *Plasma Phys. Control. Fusion* **46** S31–45
- [12] Cheng C.Z. 1992 Kinetic extensions of magnetohydrodynamic models for axisymmetric toroidal plasmas *Phys. Rep. A* **211** 1–51
- [13] Gorelenkov N.N., Cheng C.Z. and Fu G.Y. 1999 Fast particle finite orbit width and Larmor radius effects on low- n toroidicity induced Alfvén eigenmode excitation *Phys. Plasmas* **6** 2802
- [14] Kramer G.J. *et al* 2006 Interpretation of core localized Alfvén eigenmodes in DIII-D and Joint European Torus reversed magnetic shear plasmas *Phys. Plasmas* **13** 056104
- [15] Gryaznevich M.P. *et al* and the MAST Team 2008 *Nucl. Fusion* **48** 084003
- [16] Chapman I.T., Hua M.-D., Pinches S.D., Akers R.J., Field A.R., Graves J.P., Hastie R.J., Michael C.A. and the MAST Team 2010 *Nucl. Fusion* **50** 045007
- [17] Fredrickson E.D. *et al* 2012 Observation of global Alfvén eigenmode avalanche events on the National Spherical Torus Experiment 2012 *Nucl. Fusion* **52** 043001
- [18] Gerhardt S.P., Andre R. and Menard J.E. 2012 Exploration of the equilibrium operating space for NSTX-Upgrade *Nucl. Fusion* **52** 083020
- [19] Darrow D.S. *et al* 1997 Losses due to Alfvén Modes in TFTR *Nucl. Fusion* **37** 939